Proceedings of the ASME 2018
Dynamic Systems and Control Conference
DSCC2018
September 30-October 3, 2018, Atlanta, Georgia, USA

DSCC2018-9013

CONTROLLABILITY OF A PAIR OF SWIMMING MICROROTORS IN A BOUNDED DOMAIN AT LOW REYNOLDS NUMBER

Jake Buzhardt
Department of Mechanical Engineering
Clemson University
Clemson, SC 29634
Email: jbuzhar@g.clemson.edu

Vitaliy Fedonyuk
Department of Mechanical Engineering
Clemson University
Clemson, SC 29634
Email: vfedony@g.clemson.edu

Senbagaraman Sudarsanam
Department of Mechanical Engineering
Clemson University
Clemson, SC 29634
Email: ssudars@g.clemson.edu

Phanindra Tallapragada
Department of Mechanical Engineering
Clemson University
Clemson, SC 29634
Email: ptallap@clemson.edu

ABSTRACT

We investigate the dynamics of a pair of spinning spheres or microrotors in a fluid at low Reynolds numbers. These microrotors are each approximated by a rotlet, a fundamental singularity of the Stokes equation. Singularities of Stokes flows serve as useful theoretical models for microswimmers and micro-robots. Rotlet models of microswimmers have received less attention since a rotlet cannot generate translation by itself if the only control input is the rate of spin or strength of the rotlet. However a pair of rotlets can interact and execute net motion. In an unbounded domain of fluid, the positions of a pair of rotlets are not fully controllable due to the existence of an invariant. However, in a confined domain, we show that the positions of the pair of spheres are small time locally controllable. We show how control inputs can be constructed based on combinations of Lie brackets to move the rotlets from one point to another in the domain.

1 INTRODUCTION

The ability to precisely maneuver a micro-robot or a collection of small robots in a small scale fluid environment has enormous implications to areas such as targeted drug delivery [1–4], particle and cell manipulation [2–5], cell identification and diagnostics [6], and the fabrication of novel materials with tunable properties [7]. In recent years, magnetic microswimmers that are actuated by means of an external magnetic field have attracted much attention, in part due to the feasibility of fabrication of such robots and the easy means of actuation via a time varying external magnetic field [8–13].

The fabrication of a magnetic swimmer with a specialized geometry is necessary because of the reversibility of flow at low Reynolds numbers [14]. In general, the actuation for the microrobots is not a force that directly leads to a 'pull' or 'push', as these require large gradients of electric or magnetic fields. Instead, the actuation is in the form of a torque due to a time-varying magnetic field, which spins the swimmer. The interaction of the spinning body with the viscous forces produces a propulsive force. The mobility tensor of the swimmer, which relates the viscous forces on the swimmer to its velocity, has to possess a certain form with off-diagonal terms for viable locomotion to occur [15, 16]. A mobility tensor of this form results from geometric asymmetries of the body. For instance, a microrobot in the shape of a sphere or an ellipsoid cannot swim due to a rotating magnetic field in the absence of a boundary, as these

bodies do not possess an asymmetry that would enable locomotion. The dynamics of microswimmers with complex geometries are difficult to model due to the complexity of the associated mobility tensor which couples rotational and translational motion. Further complexity of the system emerges due to the interaction of a micro-robot with any nearby walls or boundaries.

We address this problem by investigating the motion of spherical magnetic *rotors* whose mobilities are very simple to compute. While a single spinning sphere cannot swim at all in an unbounded domain, two or more closely spaced spheres can interact hydrodynamically and swim together. Such pair swimmers with very simple geometries do not require any additional fabrication and can replace a single micro-robot with a complex geometry.

In this paper, we consider the problem of controlling the motion of two such microrotors in a confined domain. We consider a well known approximation of a spinning sphere by a two dimensional rotlet, a singularity of the Stokes equation [15–18]. The velocity field due to a spinning sphere confined to a cross-sectional plane whose normal vector is aligned with the axis of rotation and which passes through the center of the sphere can be approximated by a two-dimensional rotlet [18]. Such a model is appropriate for neutrally buoyant spheres that are constrained by some mechanism, such as a viscous film [19, 20]. Similar two-dimensional models have also been applied to systems of rotating disks [21]. The control inputs for our system are taken to be the strengths of the rotlets, which are directly proportional to the torques on the spheres due to the external magnetic field. Interestingly, we show that the motion of a pair of microrotors is fully controllable only when they swim in a confined domain (of any finite size) but not in the idealized setting of an infinite domain.

2 DYNAMICS OF TWO MICROROTORS

The Stokes equations describing the motion of a fluid at a scale where inertial forces are negligible and viscous forces dominate are

$$\begin{aligned} \nabla p &= \mu \nabla^2 \mathbf{u} \\ \nabla \cdot \mathbf{u} &= 0 \end{aligned} \tag{1}$$

subject to boundary conditions, where $\mathbf{u}$ is the velocity of the fluid and p is the pressure. Singularity solutions of the Stokes equation and linear combinations of such solutions have served as popular models for locomotion [22]. The rotlet is a singularity that describes the velocity of the fluid due to a torque exerted on it, such as due to the spin of the sphere.

2.1 Rotlets in the Unbounded Domain $\mathbb{R}^2$

The velocity field of the fluid at $\mathbf{x} \in \mathbb{R}^2$ due to a rotlet of strength $\gamma \hat{k}$ located at $\mathbf{x}_0$ is given by

$$\mathbf{u}(\mathbf{x}) = -\gamma \hat{k} \times \frac{\mathbf{x} - \mathbf{x}_0}{\|\mathbf{x} - \mathbf{x}_0\|^2}. \tag{2}$$

where $\hat{k}$ is the unit vector orthogonal to the plane of motion.

The stream lines induced by the rotlet form concentric circles around the rotlet, with the speed of the fluid along these streamlines decreasing with the distance from the rotlet. In (2), the velocity $\mathbf{u}(x)$ becomes undefined at $\mathbf{x} = \mathbf{x}_0$. This singularity manifests itself only in the tangential component of the fluid along the streamlines. That is, in the limit of $\mathbf{x} = \mathbf{x}_0$, a fluid particle collocated with the rotlet spins in place but does not move. This motivates one to consider only the desingularized component of the velocity field by assuming that the rotlet does not have a self-induced velocity [16, 18]. Therefore a single rotlet does not move.

If n rotlets are present in the domain, with the rotlet locations being $(\mathbf{x}_1, ..., \mathbf{x}_n)$, then each rotlet is advected by the velocity field induced by the other $n-1$ rotlets. The velocity of each of the rotlets is given by

$$\begin{aligned} \frac{dx_i}{dt} &= \sum_{\substack{j=1 \\ j \neq i}}^{n} \gamma_j \frac{(y_i - y_j)}{R_{ij}^2} \\ \frac{dy_i}{dt} &= \sum_{\substack{j=1 \\ j \neq i}}^{n} -\gamma_j \frac{(x_i - x_j)}{R_{ij}^2} \end{aligned} \tag{3}$$

where $R_{ij} = \sqrt{(x_i - x_j)^2 + (y_i - y_j)^2}$ is the distance between the i-th and the j-th rotlets.

Note that while the velocity of the fluid described by (2) is not continuous at the locations of the rotlets, the dynamics of the rotlets themselves are governed by C^∞ vector fields.

We will consider the specific case of the motion of two rotlets with the control inputs being the strengths of the rotlets, γ_1 and γ_2. Equation (3) defines a driftless control affine system, where the positions of the rotlets, $\xi = [x_1, y_1, x_2, y_2]^T$ evolve on the configuration manifold $\mathbb{R}^4$.

We show that regardless of the rotlet strengths, the distance between the rotlets remains invariant. This is seen through a direct calculation. Suppose R denotes the distance between the two

rotlets

$$\begin{aligned}\frac{d}{dt}R^2 &= \frac{d}{dt}((x_2-x_1)^2+(y_2-y_1)^2)\\ &= 2(x_2-x_1)(\dot{x}_2-\dot{x}_1)+2(y_2-y_1)(\dot{y}_2-\dot{y}_1)\\ &= \frac{2}{R^2}(x_2-x_1)(\gamma_1(y_2-y_1)-\gamma_2(y_1-y_2))\\ &\qquad +\frac{2}{R^2}(y_2-y_1)(-\gamma_1(x_2-x_1)+\gamma_2(x_1-x_2))\\ &= \frac{2}{R^2}(x_2-x_1)(\gamma_1+\gamma_2)(y_2-y_1)\\ &\qquad -\frac{2}{R^2}(x_2-x_1)(\gamma_1+\gamma_2)(y_2-y_1)\\ &= 0.\end{aligned}$$

This implies that the control system (3) is not fully controllable, or even locally controllable since neither rotlet can move relative to the other rotlet along the line connecting them.

2.2 Confined Domain with Circular Boundary

In [17], Meleshko and Aref have shown that the velocity at a point $\mathbf{x} = (x,y)$ in a bounded, circular domain due to a single point rotlet of strength γ located at $x = b, y = 0$ is described by the stream function

$$\psi(x,y) = \psi_1 + \psi_2 = \frac{\gamma}{2}\ln A(x,y) + \frac{\gamma}{2}\left[\ln\frac{1}{B(x,y)} + \frac{C(x,y)}{B(x,y)}\right] \quad (4)$$

where, if we convert their expression from polar to Cartesian coordinates,

$$\begin{aligned}A(x,y) &= r^2 - 2bx + b^2\\ B(x,y) &= a^2 - 2bx + \left(\frac{r^2b^2}{a^2}\right)\\ C(x,y) &= \left(1-\frac{r^2}{a^2}\right)\left(a^2-\frac{r^2b^2}{a^2}\right)\end{aligned}$$

Here, $r = \sqrt{x^2+y^2}$ and a is the radius of the circular domain. The stream function $\psi_1 = (\gamma/2)\ln(A(x,y))$ is the same as for the rotlet in the unbounded domain $\mathbb{R}^2$ and the stream function $\psi_2 = (\gamma/2)(1/B(x,y) + C(x,y)/B(x,y))$ is due to a system of image singularities placed outside the circular domain. The combined stream function ψ produces a fluid velocity field that satisfies the boundary condition of zero normal and tangential velocity on the boundary. Differentiating (4) gives the velocity field due to a single rotlet.

The velocity of the fluid at a point (x,y) due to a rotlet of strength γ_1 located at (x_1,y_1) is obtained by a rotation transformation

$$\mathbf{u}(x,y) = \mathbf{R^{-1}}(\theta_1)\frac{\gamma_1}{2}\begin{bmatrix}\frac{(\frac{B}{A})(BA_y-AB_y)}{B^2} + \frac{BC_y-CB_y}{B^2}\\ \frac{-(\frac{B}{A})(BA_x-AB_x)}{B^2} - \frac{BC_x-CB_x}{B^2}\end{bmatrix} \quad (5)$$

where A_x, B_x, C_x and A_y, B_y, C_y denote the partial derivatives of the functions with respect to x_b and y_b respectively with $\mathbf{x}_b = \mathbf{R}(\theta_1)\mathbf{x}$. Here $\theta_1 = \arctan(y_1/x_1)$ and $\mathbf{R}(\theta_1)$ is the rotation matrix,

$$\mathbf{R}(\theta_1) = \begin{pmatrix}\cos\theta_1 & \sin\theta_1\\ -\sin\theta_1 & \cos\theta_1\end{pmatrix}$$

that transforms the system to a coordinate system in which the rotlet lies on the positive x-axis at $b = \sqrt{x_1^2+y_1^2}$. The velocity of the fluid $\mathbf{u}$ is zero if $x^2+y^2 = a^2$.

As in the case of the unbounded domain, the velocity of the rotlet is desingularized, i.e. a rotlet does not induce a velocity on itself. However the image singularities do induce a velocity to the rotlet,

$$\begin{bmatrix}\frac{dx_1}{dt}\\ \frac{dy_1}{dt}\end{bmatrix} = \mathbf{R^{-1}}(\theta_1)\frac{\gamma_1}{2}\begin{bmatrix}\frac{-B_y}{B} + \frac{BC_y-CB_y}{B^2}\\ \frac{B_x}{B} - \frac{BC_x-CB_x}{B^2}\end{bmatrix}. \quad (6)$$

When n rotlets are present in the circular domain, the velocity of the i-th rotlet is the sum of the velocities induced by its own image singularities, the other $n-1$ rotlets, and the image systems of the other $n-1$ rotlets. In particular, the governing equations for the motion of two rotlets of strengths γ_1 and γ_2 respectively, in the circular domain are

$$\begin{bmatrix}\frac{dx_i}{dt}\\ \frac{dy_i}{dt}\end{bmatrix} = \sum_{\substack{j=1\\ j\neq i}}^{2}\mathbf{R^{-1}}(\theta_j)\frac{\gamma_j}{2}\begin{bmatrix}\frac{(\frac{B}{A})(BA_y-AB_y)}{B^2} + \frac{BC_y-CB_y}{B^2}\\ \frac{-(\frac{B}{A})(BA_x-AB_x)}{B^2} - \frac{BC_x-CB_x}{B^2}\end{bmatrix}$$

$$+\ \mathbf{R^{-1}}(\theta_i)\frac{\gamma_i}{2}\begin{bmatrix}\frac{-B_y}{B} + \frac{BC_y-CB_y}{B^2}\\ \frac{B_x}{B} - \frac{BC_x-CB_x}{B^2}\end{bmatrix} \quad (7)$$

3 CONTROLLABILITY

The position of the two rotlets parameterized by $\xi = [x_1, y_1, x_2, y_2]^T$ evolves on the configuration manifold $\mathbb{Q} = \{(x_1, y_1, x_2, y_2) \in \mathbb{R}^4 | x_1^2 + y_1^2 \leq a^2 \wedge x_2^2 + y_2^2 \leq a^2\}$. The tangent space at any point $\xi \in \mathbb{Q}$ will be denoted by $T_\xi \mathbb{Q}$. The governing equation (7) for the motion of the rotlets is a driftless control affine system, Σ, with the strengths of the rotlets being the control inputs u_1 and u_2

$$\Sigma: \quad \dot{\xi} = g_1(\xi)u_1 + g_2(\xi)u_2 \tag{8}$$

where g_1 and g_2 are C^∞ vector fields and $u_1 \in \mathbb{R}$ and $u_2 \in \mathbb{R}$. Here each of the the vector fields $g_i(\xi)$ is a column vector whose elements are the coefficients of γ_i from (7).

3.1 SMALL-TIME LOCAL CONTROLLABILITY

We first show that the two rotlets can move in any direction from almost any initial positions in an arbitrarily small time, i.e.for almost any initial state ξ_0 of the control system Σ, and small enough time t_0, the reachable set $R_\Sigma(t < t_0, \xi_0)$ contains a neighborhood of ξ_0. This is shown using the Lie algebra rank condition (LARC) [23–26].

Given two vector fields, g_i and g_j the Lie bracket, denoted $[\, g_i, g_j \,]$ is defined as

$$[\, g_i, g_j \,] = \nabla g_j \, g_i - \nabla g_i \, g_j.$$

This Lie bracket can be interpreted as the infinitesimal motion that results from flowing in the sequence of directions $g_i \, , g_j \, , -g_i \, , -g_j$. Associated with Σ is a distribution

$$\Delta = \text{span}\{g_1, g_2\}$$

whose closure under Lie bracketing we denote by $\bar{\Delta}$. By Chow's theorem, the system Σ of (8) is locally controllable at a point $\xi \in \mathbb{Q}$ if $\dim(\bar{\Delta}_\xi) = \dim(T_\xi \mathbb{Q})$ [23–26]. This conclusion of nonlinear control theory allows us to evaluate whether a system is small time locally controllable (STLC) at a point ξ by checking the rank of the Lie algebra $\bar{\Delta}_\xi$. This is called the Lie algebra rank condition (LARC). We also note that for drift-free systems such as Σ, small-time local controllability implies controllability [23].

To evaluate the controllability of a system of two rotlets in a confined circular domain, we apply the LARC to (7). Through computations in MAPLE it was found that there exists a nonempty subset $C \subseteq \mathbb{Q}$ in which the system is STLC. Specifically, by numerically evaluating a set of Lie brackets for $10,000$ different values of ξ we find that the vector fields

$$\begin{array}{l} g_1 \\ g_2 \\ [\, g_1, g_2 \,] \\ [\, g_1, [\, g_1, g_2 \,] \,] \end{array} \tag{9}$$

span the tangent space $T_\xi \mathbb{Q} = R^4$ at all points $\xi \in \mathbb{Q}$ except the special configurations in which both rotlets lie on a chord passing through the center of the circular domain. Therefore, from any initial configuration $\xi_0 \in C$, the system of two rotlets can be driven in any direction in an arbitrarily small amount of time through a motion generated by the Lie brackets given in (9).

Note that the system may still be STLC for $\xi \in \mathbb{Q} \setminus C$. For initial conditions in $\mathbb{Q} \setminus C$, the vector fields g_1, g_2, $[g_1, g_2]$ are linearly independent. Since we only consider the brackets of (9), it is possible that there exists a Lie bracket of higher order that is linearly independent of the vector fields g_1, g_2, $[g_1, g_2]$.

4 Simulation of Lie Brackets

Now that it has been shown that for most configurations, four linearly independent vector fields from the Lie algebra can be found to span the tangent space, an additional difficulty remains in using the control inputs γ_1 and γ_2 to generate the motions associated with each of these vector fields.

The motion associated with the vector field g_1 is readily simulated, as it corresponds to the case where $\gamma_2 = 0$ and $\gamma_1 \neq 0$. The resulting motion, found by integrating (7) from an initial configuration $\xi_0 \in C$ is depicted in Figure 1. Similarly, the motion associated with the vector field g_2 is simulated by integrating (7) for the case where $\gamma_1 = 0$ and $\gamma_2 \neq 0$. This result is depicted in Figure 2.

The motion given by the vector field $[g_1, g_2]$ is not as simply simulated. To produce this motion, we consider the interpretation of the Lie bracket as the infinitesimal motion produced by flowing in the sequence of directions $g_1 \, , g_2 \, , -g_1 \, , -g_2$. With this, the motion is numerically simulated by cycling through this sequence of inputs over a period of 1 time unit. The resulting motion over an interval of 50 periods is shown in Fig. 3.

The motion given by the vector field $[g_1, [g_1, g_2]]$ is simulated using a similar strategy by flowing in the sequence of directions specified by $g_1 \, , [g_1, g_2] \, , -g_1 \, , -[g_1, g_2]$ over a period of one time unit. In the $[\, g_1, g_2 \,]$ portions of this sequence, the input cycles through the sequence for the $[g_1, g_2]$ bracket with a frequency four times higher than the frequency of changing inputs in the $[g_1, [g_1, g_2]]$ sequence. The resulting motion over an interval of 50 periods is shown in Fig. 4.

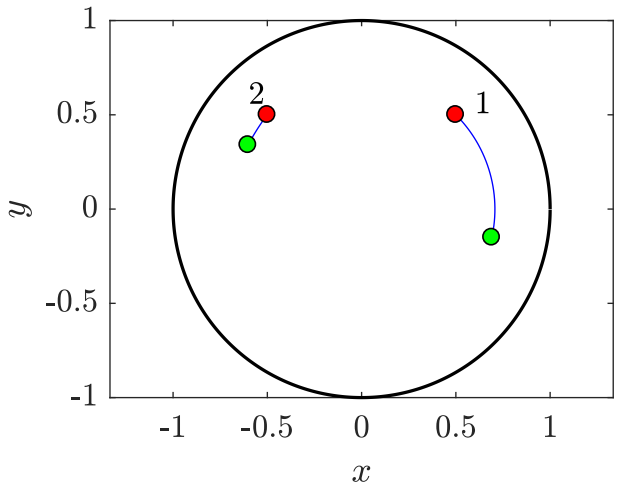

FIGURE 1: SIMULATION OF ROTLET MOTION ALONG THE VECTOR FIELD g_1, WHICH CORRESPONDS TO THE INPUT $\gamma_1 = 1$ AND $\gamma_2 = 0$ FOR ONE TIME UNIT FROM AN INITIAL CONFIGURATION $\xi = [0.5\ ,\ 0.5\ ,\ -0.5\ ,\ 0.5]^T$, DEPICTED BY RED MARKERS.

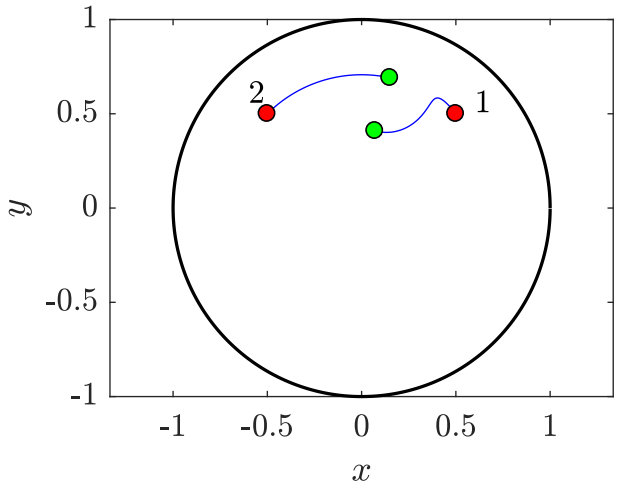

FIGURE 2: SIMULATION OF ROTLET MOTION ALONG THE VECTOR FIELD g_2, WHICH CORRESPONDS TO THE INPUT $\gamma_1 = 0$ AND $\gamma_2 = 1$ FOR ONE TIME UNIT FROM AN INITIAL CONFIGURATION $\xi = [0.5\ ,\ 0.5\ ,\ -0.5\ ,\ 0.5]^T$, DEPICTED BY RED MARKERS.

4.1 Motion in a Given Direction

It has been shown that the vector fields given by the Lie brackets in (9) span the tangent space $T_{\xi_0}\mathbb{Q}$ associated with the system Σ of (8) at any configuration $\xi_0 \in C$, and thus Σ is locally controllable from these configurations. Therefore, a motion in the direction of any vector $v \in T_{\xi_0}\mathbb{Q}$ may be generated by some linear combination of the Lie brackets that span the tangent space. With the Lie brackets given in (9) we can write

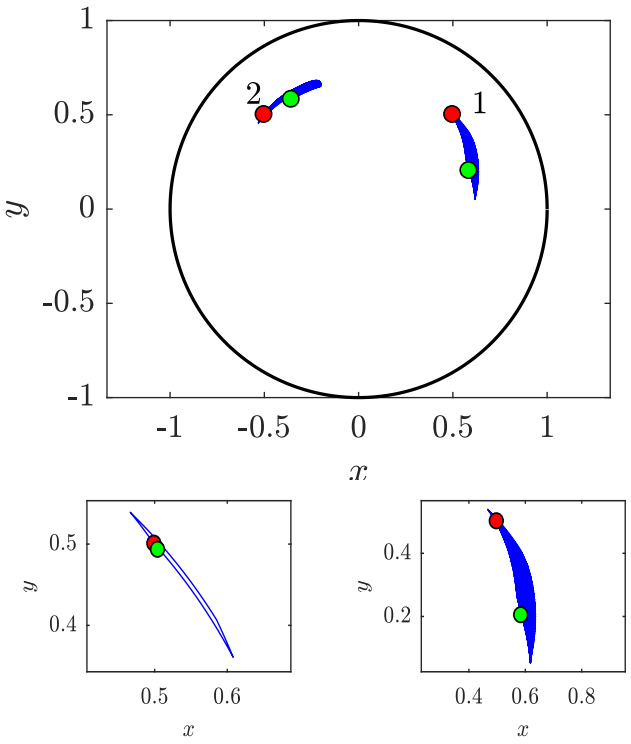

FIGURE 3: ROTLET MOTION DUE TO $[g_1, g_2]$ FOR 50 TIME UNITS FROM AN INITIAL CONFIGURATION $\xi_0 = [0.5\ ,\ 0.5\ ,\ -0.5\ ,\ 0.5]^T$, DEPICTED BY RED MARKERS. THE LEFT SUBFIGURE DEPICTS THE MOTION OF ROTLET 1 FOR ONE CYCLE COMPOSED OF FLOWS ALONG $g_1\ ,\ g_2\ ,\ -g_1\ ,\ -g_2$ FOR 1 TIME UNIT TOTAL. THE RIGHT SUBFIGURE DEPICTS THE MOTION OF ROTLET 1 FOR 50 SUCH CYCLES.

$$v = a_1 g_1 + a_2 g_2 + a_3 [\, g_1, g_2\,] + a_4 [\, g_1, [\, g_1, g_2\,]\,] \tag{10}$$

or, in matrix form

$$v = G(\xi_0)\, a$$

where $G(\xi_0)$ is the matrix with columns given by the vector fields in (9) evaluated at the initial configuration ξ_0 and a is a vector of coefficients. While the matrix $G(\xi_0)$ depends on the initial configuration, we have shown that it has full rank for any $\xi_0 \in C$. Therefore, $G(\xi_0)$ is invertible and we can solve for the coefficients needed to achieve motion in an arbitrary direction $v \in T_{\xi_0}\mathbb{Q}$

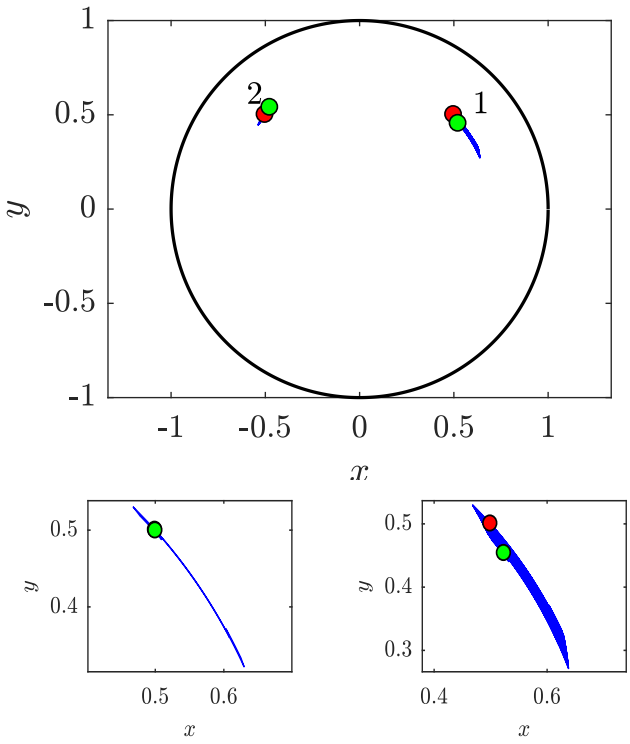

FIGURE 4: ROTLET MOTION DUE TO $[g_1,[g_1,g_2]]$ FOR 50 TIME UNITS FROM AN INITIAL CONFIGURATION $\xi_0 = [0.5\ ,\ 0.5\ ,\ -0.5\ ,\ 0.5]^T$, DEPICTED BY RED MARKERS. THE LEFT SUBFIGURE DEPICTS THE MOTION OF ROTLET 1 FOR ONE CYCLE COMPOSED OF FLOWS ALONG $g_1,\ [g_1,g_2],-g_1,-[g_1,g_2]$ FOR 1 TIME UNIT TOTAL. THE RIGHT SUBFIGURE DEPICTS THE MOTION OF ROTLET 1 FOR 50 SUCH CYCLES.

as

$$a = [G(\xi_0)]^{-1}\, v \tag{11}$$

Solving this equation yields the linear combination of the vector fields that is required to instantaneously steer the system from a given state in the direction specified by $v \in T_{\xi_0}\mathbb{Q}$.

As a concrete example, we consider the system at the beginning state shown in Figs. 1 - 3, where

$$\xi_0 = [0.5 \quad 0.5 \quad -0.5 \quad 0.5]^T$$

in a domain bounded by a circle of radius $a = 1$. If we wish to instantaneously steer the system in the direction specified by

$$v = [1 \quad 0 \quad 0 \quad 0]^T$$

which corresponds to motion of rotor 1 in a direction parallel to the x-axis, then from (11) we find the coefficients of each vector field needed for this motion to be

$$a \approx [6.69 \quad 9.20 \quad -183. \quad 11.2]^T$$

5 CONCLUSION

Rotlets serve as a convenient mathematical approximation for realizable physical systems, such as spheres spinning in a low Reynolds number flow due to the presence of a rotating magnetic field. A single rotlet cannot generate a translation in an unbounded domain and while they can move in a confined domain, such as a circular region, this motion is not controllable. We have shown that due to the existence of an invariant, the motion of a system of two rotlets is uncontrollable in the idealized setting of an unbounded domain. However, through numerical computations and the application of the Lie algebra rank condition, we have shown that a comparable system of two rotlets in a bounded, circular domain is controllable due to the presence of a boundary. This finding implies that spherical microrobots, which are easily fabricated, can move as pairs in a controllable fashion, even though individually they cannot. Furthermore, the model used herein of the rotlet in the presence of a boundary is more representative of a physical system than the idealized model of an unbounded domain. Therefore, this mathematical finding implies that such a physical system can be controlled by varying the inputs systematically in accordance with an appropriate set of Lie brackets.

Potential future directions of study include path planning for bodies with more complex geometries, which could improve the controllability of the system by introducing additional asymmetries.

REFERENCES

[1] Nelson, B. J., Kaliakatsos, I. K., and Abbott, J. J., 2010. "Microrobots for minimally invasive medicine". *Annual Review of Biomedical Engineering,* ***12***, pp. 55–85.

[2] Zhang, L., Petit, T., Peyer, K. E., and Nelson, B. J., 2012. "Targeted cargo delivery using a rotating nickel nanowire". *Nanomedicine,* ***8***(7), pp. 1074–80.

[3] Peyer, K. E., Zhang, L., and Nelson, B. J., 2013. "Bio-inspired magnetic swimming microrobots for biomedical applications". *Nanoscale,* ***4***(5), pp. 1259–1272.

[4] Gao, W., Kagan, D., Clawson, C., Campuzano, S., Chuluun-Erdene, E., Shipton, E., Fullerton, E., Zhang, L., Lauga, E., and Wang, J., 2012. "Cargo-towing fuel-free magnetic nanoswimmers for targeted drug delivery". *Small*.

[5] Petit, T., Zhang, L., Peyer, K. E., Kratochvil, B. E., and Nelson, B. J., 2012. "Selective trapping and manipulation

of microscale objects using mobile microvortices". *Nano Letters,* ***12***(1), p. 156160.

[6] Ding, Y., Qiu, F., Solvas, X. C., Chiu, F. W. Y., Nelson, B. J., and de Mello, A., 2016. "Microfluidic-based droplet and cell manipulations using artificial bacterial flagella". *Micromachines,* ***7***(2), p. 25.

[7] Snezhko, A., and Aranson, I. S., 2011. "Magnetic manipulation of self-assembled colloidal asters". *Nature materials,* ***10***, pp. 698–703.

[8] Dreyfus, R., Baudry, J., Roper, M. L., Fermigier, M., Stone, H. A., and Bibette, J., 2005. "Microscopic artificial swimmers". *Nature*.

[9] Zhang, L., Abbott, J. J., Dong, L., Kratochvil, B. E., Bell, D., and Nelson, B. J., 2009. "Artificial bacterial flagella: Fabrication and magnetic control". *Applied Physics Letters,* ***94***, p. 064107.

[10] Ghosh, A., Mandal, P., Karmakar, S., and Ghosh, A., 2013. "Analytical theory and stability analysis of an elongated nanoscale object under external torque". *Physical Chemistry Chemical Physics,* ***15***, p. 10817.

[11] Cheang, U. K., Meshkati, F., Kim, D., Kim, M. J., and Fu, H. C., 2014. "Minimal geometric requirements for micropropulsion via magnetic rotation". *Physical Review E*.

[12] Meshkati, F., and Fu, H., 2014. "Modeling rigid magnetically rotated microswimmers: Rotation axes, bistability, and controllability". *Physical Review E,* ***90***(6), p. 063006.

[13] Chen, X. Z., Hoop, M., Mushtaq, F., Siringil, E., Hu, C., J.Nelson, B., and Pané, S., 2017. "Recent developments in magnetically driven micro- and nanorobots". *Applied Materials Today,* ***9***, pp. 37–48.

[14] Purcell, E. M., 1977. "Life at low reynolds number". *American Journal of Physics,* ***45***, pp. 3–11.

[15] Happel, J., and Brenner, H., 1983. *Low Reynolds number hydrodynamics: with special applications to particulate media (Mechanics of Fluids and Transport Processes)*. Springer.

[16] Kim, S., and Karrila, S. J., 2005. *Microhydrodynamics: Principles and Selected Applications*. Dover Publications.

[17] Meleshko, V. V., and Aref, H., 1996. "A blinking rotlet model for chaotic advection". *Physics of Fluids*(8), p. 3215.

[18] Lushi, E., and Vlahovska, P. M., 2015. "Periodic and chaotic orbits of plane-confined micro-rotors in creeping flows". *Journal of Nonlinear Science,* ***25***(5), p. 11111123.

[19] Leoni, M., and Liverpool, T. B., 2010. "Dynamics and interactions of active rotors". *EPL (Europhysics Letters),* ***92***(6), p. 64004.

[20] Fily, Y., Baskaran, A., and Marchetti, M., 2012. "Cooperative self-propulsion of active and passive rotors". *Soft Matter,* ***8***, pp. 3002–3009.

[21] Grzybowski, B. A., Stone, H., and Whitesides, G., 2002. "Dynamics of self assembly of magnetized disks rotating at the liquid–air interface". *PNAS,* ***99***(7), pp. 4147–4151.

[22] Lauga, E., and Powers, 2009. "The hydrodynamics of swimming microorganisms". *Reports on Progress in Physics,* ***72***(9), p. 096601.

[23] Murray, R., Li, Z., and Sastry, S. S., 1994. *A Mathematical Introduction to Robotic Manipulation*. CRC Press.

[24] Sastry, S., 1999. *Nonlinear Systems: Analysis, Stability, and Control*. Springer Verlag-Berlin.

[25] Bullo, F., and Lewis, A. D., 2004. *Geometric Control of Mechanical Systems*. Springer Verlag-Berlin.

[26] Bloch, A. M., 2003. *Nonholonomic Mechanics and Control*. Springer Verlag.